

# Activation of BNGR-A24 by Direct Interaction with Tachykinin-Related Peptides from the Silkworm *Bombyx mori* Leads to the G<sub>q</sub>- and G<sub>s</sub>-Coupled Signaling Cascades

Xiaobai He,<sup>†</sup> Jiashu Zang,<sup>†</sup> Xiangmei Li,<sup>‡</sup> Jiajie Shao,<sup>†</sup> Huipeng Yang,<sup>†</sup> Jingwen Yang,<sup>§</sup> Haishan Huang,<sup>||</sup> Linjie Chen,<sup>†</sup> Liangen Shi,<sup>§</sup> Chenggang Zhu,<sup>†</sup> Guozheng Zhang,<sup>\*,‡</sup> and Naiming Zhou<sup>\*,†</sup>

<sup>†</sup>Institute of Biochemistry, College of Life Sciences, Zhejiang University, Zijingang Campus, Hangzhou, Zhejiang 310058, China

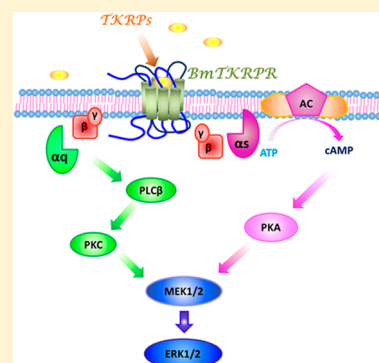
<sup>‡</sup>Key Laboratory of Genetic Improvement of Sericulture, Ministry of Agriculture, Jiangsu University of Science and Technology, Zhenjiang, Jiangsu 212018, China

<sup>§</sup>Department of Economic Zoology, College of Animal Sciences, Zhejiang University, Zijingang Campus, Hangzhou, Zhejiang 310058, China

<sup>||</sup>Zhejiang Provincial Key Laboratory for Technology and Application of Model Organisms, School of Life Sciences, Wenzhou Medical University, Wenzhou, Zhejiang, China

## S Supporting Information

**ABSTRACT:** Tachykinins constitute one of the largest peptide families in the animal kingdom and exert their diverse actions via G protein-coupled receptors (GPCRs). In this study, the *Bombyx* tachykinin-related peptides (TKRPs) were identified as specific endogenous ligands for the *Bombyx* neuropeptide GPCR A24 (BNGR-A24) and thus designated BNGR-A24 as BmTKRPR. Using both mammalian cell line HEK293 and insect cell line Sf21, further characterization demonstrated that BmTKRPR was activated, thus resulting in intracellular accumulation of cAMP, Ca<sup>2+</sup> mobilization, and ERK1/2 phosphorylation in a G<sub>s</sub> and G<sub>q</sub> inhibitor-sensitive manner. Moreover, quantitative reverse transcriptase polymerase chain reaction analysis and dsRNA-mediated knock-down experiments suggested a possible role for BmTKRPR in the regulation of feeding and growth. Our findings enhance the understanding of the *Bombyx* TKRP system in the regulation of fundamental physiological processes.



Tachykinin-related peptides (TKRPs), orthologs of tachykinin in vertebrates, were originally identified as myotropic peptides from the central nervous system (CNS) of *Locusta migratoria*.<sup>1,2</sup> They were subsequently discovered in *Leucophaea maderae*,<sup>3,4</sup> *Calliphora vomitoria*,<sup>5</sup> *Culex salinarius*,<sup>6</sup> *Drosophila melanogaster*,<sup>7</sup> and *Apis mellifera*.<sup>8</sup> The majority of insect tachykinins share the same Phe-X1-Gly/Ala-X2-Arg-NH<sub>2</sub> motif in their C-terminal consensus sequence. This motif is highly analogous to the vertebrate TK common motif.<sup>9,10</sup> Tachykinins have been found to play various physiological roles in neuromodulation and gut activity.<sup>11–15</sup> In *Bombyx mori*, a cDNA encoding six different TKRP peptides was identified by searching *in silico*,<sup>16,17</sup> and five mature TKRP peptides were detected in the brain of silkworms at the larval, pupal, and adult stages by peptidomics analysis.<sup>18</sup>

The receptor for the tachykinin-related peptide was first identified as a typical G protein-coupled receptor (GPCR) from *D. melanogaster*, termed the *Drosophila* tachykinin receptor (DTKR and CG7887);<sup>19</sup> subsequently, the *Drosophila* neurokinin receptor (NKD and CG6515),<sup>20</sup> stable fly (*Stomoxys calcitrans*) tachykinin-related peptide receptor (STKR),<sup>21</sup> and putative cockroach (*L. maderae*) tachykinin receptor (LTKR)<sup>22</sup> were identified. Functional analysis demonstrated that DTKR

and STKR were activated by tachykinin-related peptides, thus triggering intracellular Ca<sup>2+</sup> mobilization and secondary cAMP accumulation.<sup>19,23,24</sup> However, the corresponding receptors for insect TKRPs, together with other related signaling information, remain to be further elucidated.

Three putative tachykinin receptor orthologs, BNGR-A24, -A32, and -A33, have been identified from the *Bombyx* genome by genomic data mining and phylogenetic analysis.<sup>16,25,26</sup> BNGR-A32 and BNGR-A33, together with *Drosophila* NKD, were most recently identified as receptors for insect natalins (NTLs). These are arthropod-specific neuropeptides with a conserved F/YxxxR-amide C-terminal motif that is closely related to that of the TKRPs. NTLs have been suggested to have a possible role in the regulation of reproduction.<sup>27</sup> In the study presented here, we report the cloning of cDNAs encoding the putative tachykinin-related peptide receptor BNGR-A24 from the brain of a silkworm, *B. mori*, as well as the functional expression of this receptor in human embryonic kidney 293 (HEK293) and insect *Spodoptera frugiperda* (Sf21)

Received: June 10, 2014

Revised: October 2, 2014

Published: October 2, 2014

cell lines. Further characterization of both binding and signaling led us to conclude that BNGR-A24 was specifically activated by TKRPs with high affinity.

## MATERIALS AND METHODS

**Materials.** Larvae of the silkworm strain p50 were kindly provided by G. Zhang. Sf21 cell lines were kindly provided by Z. Zhang. X-tremeGENE HP was purchased from Roche (Mannheim, Germany). The membrane probe DiI, RIPA lysis buffer, and horseradish peroxidase-conjugated secondary antibody were purchased from Beyotime (Haimen, China). UBO-QIC was purchased from E. Kostenis (University of Bonn, Bonn, Germany). TKRPs and Cy5-tagged TKRP5 (Cy5-TKRPs) were synthesized by Biopeptek Biochem Ltd. (Qingdao, China). Anti-phospho-ERK1/2 (Thr202/Tyr204) and anti-ERK1/2 (p44/42 MAPK) rabbit antibodies and HRP substrate were all purchased from Cell Signaling Technology (Danvers, MA).

**Molecular Cloning and Plasmid Construction.** Total RNA was isolated from the brain of *B. mori* larva using the RNAiso Plus reagent (Takara) following the manufacturer's instructions. cDNA was synthesized using a PrimeScript 1st Strand cDNA Synthesis Kit (Takara) according to the manufacturer's instructions. The entire coding region of the BNGR-A24 gene was cloned and sequenced. The primers used for BNGR-A24 synthesis were 5'-ATGATG CTGGAC GAGCTC GGGC-3' (forward) and 5'-TTACAT ACTTGT TCCGTT CTTTCG G-3' (reverse). The obtained PCR products were directionally cloned into the pCMV-Flag vector and the pEGFP-N1 vector for expression in mammalian cells. To express in insect cells, the immediate-early gene promoter (IE1) and homologous region 3 (Hr3) of *B. mori* nucleopolyhedrovirus (BmNPV) and the promoter of BmAcitnA3 were used to replace the corresponding sites of pCMV-Flag and pEGFP-N1 as previously described.<sup>28</sup> pBmCRE-Luc was also reconstructed using the promoter of BmHsp20.4 (*B. mori* heat shock protein 20.4, GenBank accession number EU350577) and the BmFibL (*B. mori* fibroin light chain, GenBank accession number NM\_001044023) polyadenylation signal to replace pVIP (promoter of vaso-intestinal peptide) and the SV40 polyadenylation signal of pCRE-Luc, respectively. All constructs were sequenced to verify the correct sequences and orientations.

**Cell Culture and Transfection.** The human embryonic kidney cell line (HEK293) cells were maintained in DMEM supplemented with 10% fetal bovine serum (Hyclone) and 4 mM L-glutamine (Invitrogen) at 37 °C in a humidified incubator containing 5% CO<sub>2</sub>. The insect *S. frugiperda* ovarian cell line Sf21 cells were maintained in TC100 insect medium (Applichem, Darmstadt, Germany) supplemented with 10% fetal bovine serum (Pufei, Shanghai, China) at 28 °C. To establish stable HEK-BNGR-A24 (HEK293-BmTKRPR) and Sf21-BNGR-A24 (Sf21-BmTKRPR) cell lines, HEK293 cells, and Sf21 cells were seeded in six-well plates and transfected with 2 µg of BNGR-A24 plasmid using X-tremeGENE HP according to the manufacturer's instructions. Twenty-four hours later, transfected cells were reseeded in 100 mm dishes and selected with complete medium and 800 mg/L G418. When needed, HEK293 and Sf21 cells were transiently cotransfected with 2 µg of BNGR-A24 plasmid and 0.5 µg of the corresponding reporter gene pCRE-luc or pBmCRE-luc.

**Detection of cAMP Response Element Binding Protein (CREB) Activity.** A reporter gene assay was

performed to investigate changes in the intracellular levels of cAMP. A pCRE-Luc or pBmCRE-Luc reporter gene system consisting of the firefly luciferase coding region under the control of a minimal promoter containing cAMP response elements was used to measure intracellular cAMP levels. HEK293 and Sf21 cells transiently cotransfected with BNGR-A24 and the reporter protein were seeded into 96-well plates and incubated overnight. Cells were then stimulated with different concentrations of neuropeptides in serum-free medium and incubated for 4 h. Luciferase activity was detected using a firefly luciferase assay kit (Ken-real, Shanghai, China). When required, cells were treated with pertussis toxin (PTX, 50 ng mL<sup>-1</sup>) for 16 h or cholera toxin (CT, 100 ng mL<sup>-1</sup>) for 2 h prior to the start of the experiment.

**Measurement of the Accumulation of cAMP.** Cells were cultured in 24-well plates overnight and pretreated with the PDE inhibitor IBMX (300 µM) for 1 h, followed by incubation with TKRP1 (100 nM) or forskolin (FSK, 10 µM) for 15 min. The reaction was terminated through the removal of medium, the addition of ice-cold PBS, and a single wash. Cells were lysed, and cAMP formation was determined using a competitive binding technique based on an enzyme-linked immunosorbent assay (ELISA) (Parameter cAMP assay, R&D, Minneapolis, MN) according to the manufacturer's instructions. The results were expressed as the concentration of cAMP in the supernatants.

**Intracellular Calcium Measurement.** The fluorescent Ca<sup>2+</sup> indicator fura-2 was employed to monitor changes in intracellular calcium. HEK293-BNGR-A24 cells were harvested with a Nonenzymatic Cell Dissociation Solution (M&C Gene Technology), washed twice with phosphate-buffered saline, and resuspended at a density of 5 × 10<sup>6</sup> cells mL<sup>-1</sup> in Hanks' balanced salt solution containing 0.025% bovine serum albumin. The cells were then loaded with 3 µM Fura-2-AM (Dojindo Laboratories) for 30 min at 37 °C. For Sf21-BNGR-A24 cells, the experiment was performed at 28 °C in HBM {Hepesec-Buffered Medium [140 mM NaCl, 5 mM KCl, 1 mM MgCl<sub>2</sub>, 1.2 mM Na<sub>2</sub>HPO<sub>4</sub>, 5 mM NaHCO<sub>3</sub>, 10 mM glucose, and 20 mM HEPES-NaOH, CaCl<sub>2</sub> (1 mM) (pH 6.2)]} instead of Hank's solution. Calcium flux was measured using excitation wavelengths of 340 and 380 nm in a fluorescence spectrometer (Tecan Infinite 200 PRO). When required, cells were treated for 30 min with U73122 or UBO-QIC prior to the initiation of the experiment.

**ERK1/2 Activation Assay.** HEK293-BNGR-A24 cells were seeded in 24-well plates and starved for 1 h in serum-free medium to reduce the level of background ERK1/2 activation and to eliminate the effects of the change of medium. After stimulation with TKRPs, cells were lysed using RIPA buffer. Equal amounts of total cell lysates were size-fractionated via sodium dodecyl sulfate–polyacrylamide gel electrophoresis (SDS–PAGE) (10%) and transferred to a PVDF membrane (Millipore). Membranes were blocked in blocking buffer (TBS containing 0.05–0.1% Tween 20 and 5% nonfat dry milk) for 1 h at room temperature (RT) and then probed with rabbit monoclonal anti-phospho-ERK1/2 antibody, followed by detection using an anti-rabbit HRP-conjugated second antibody according to the manufacturers' protocols. Total ERK1/2 was assessed as a loading control after p-ERK1/2 chemiluminescence detection using HRP substrate. The levels of ERK1/2 phosphorylation were normalized to total ERK1/2, and all immunoblots were quantified using the Bio-Rad Quantity One imaging system.

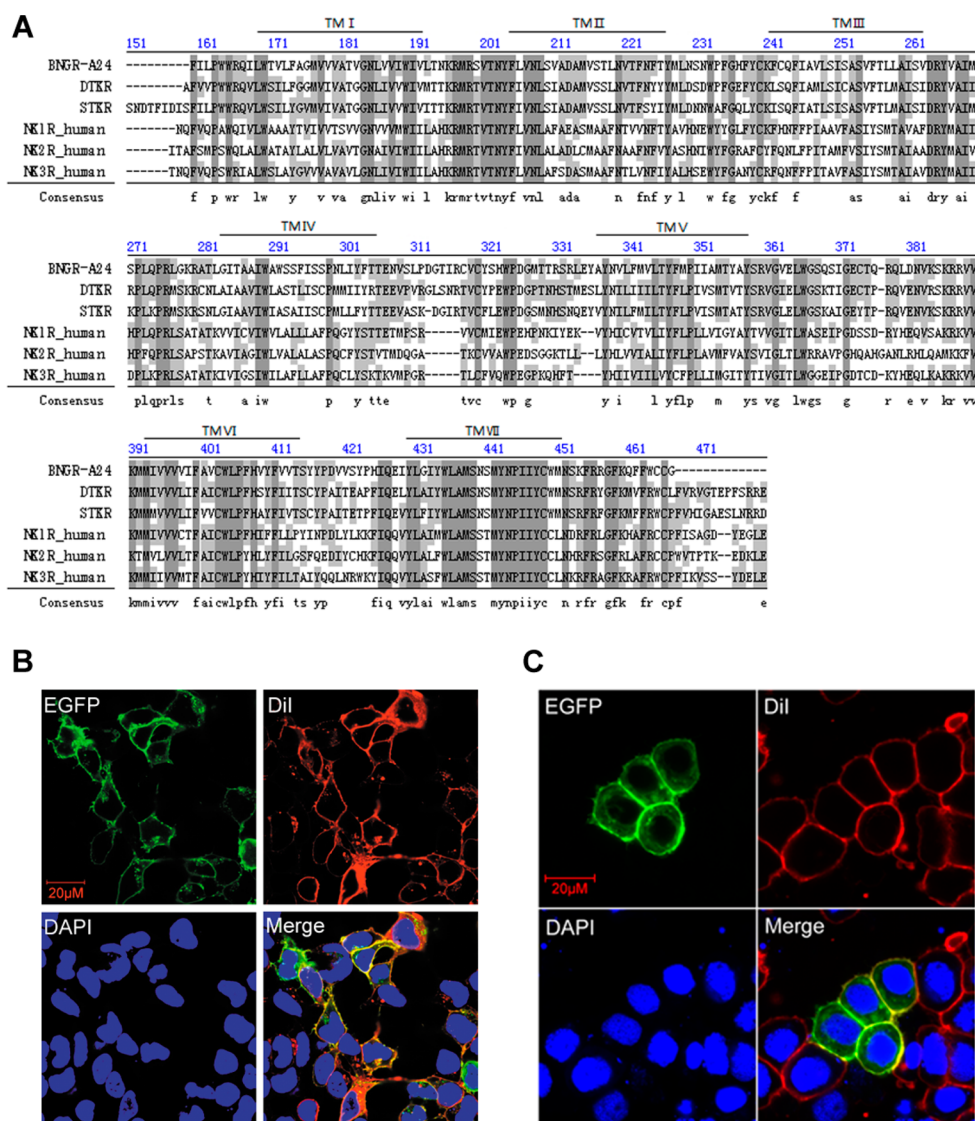


**Figure 1.** Cloning and expression of BNGR-A24 in HEK293 and Sf21 cells. (A) Alignment of the amino acid sequences from insect (STKR, DTKR, and BNGR-A24) and human (NK-1–3 receptors) tachykinin-like receptors. Highly divergent N- and C-terminal sequence parts are not displayed. Identically conserved residues are indicated below the sequences. Seven putative transmembrane regions (TM1–7) are indicated above the corresponding sequence parts. (B and C) HEK293 cells (B) and Sf21 cells (C) stably expressing EGFP-tagged BNGR-A24 were stained with a plasma membrane probe (DiI) and a nuclear probe (DAPI) and detected by confocal microscopy. All data were taken from at least three independent experiments.

**Confocal Microscopy.** For expression analysis of the receptor at the cell surface, HEK293 cells and Sf21 cells transiently or stably expressing receptor EGFP were seeded in cover glass-bottomed six-well plates. Cells were washed with PBS and fixed with 3% paraformaldehyde in PBS for 10 min at room temperature. To detect the expression of receptors on the cell membrane, cells were stained with the membrane probe DiI for 5–10 min, and after fixation with 3% paraformaldehyde, the cells were incubated with DAPI (Invitrogen) for 10 min to stain the cell nuclei. The cells were mounted in 50% glycerol and visualized by fluorescence microscopy using a Zeiss LSM510 laser scanning confocal microscope attached to a Zeiss Axiovert 200 microscope with a Zeiss Plan-Apo 63X, 1.40 NA oil immersion lens. Images were collected using LSM 5 Image Examiner and processed with Adobe Photoshop.

**Binding Assay.** HEK293 and Sf21 cells stably expressing the BNGR-A24 construct were detached as described in

Intracellular Calcium Measurement and resuspended at a density of  $5 \times 10^6$  cells  $\text{mL}^{-1}$  in cold PBS supplemented with 0.25% BSA (FACS buffer). Samples of labeled and unlabeled peptides were made in FACS buffer at a concentration 3 times the final concentration specified. A 200  $\mu\text{L}$  volume of labeled ligand and 200  $\mu\text{L}$  of buffer or unlabeled ligand were added to 200  $\mu\text{L}$  of cells. After incubation on ice for 90 min, the cells were pelleted and washed three times in FACS buffer. The cells were then resuspended and fixed with 1% paraformaldehyde in FACS buffer for 15 min. Binding was assessed by measuring the fluorescence intensity with an FACScan flow cytometer (Beckman) and is presented as the percentage of total binding. The binding displacement curves were analyzed with GraphPad Prism.

**In Vitro dsRNA Synthesis and Injection.** The templates used for the preparation of dsRNA were the PCR-derived fragments sandwiched by two T7 promoter sequences

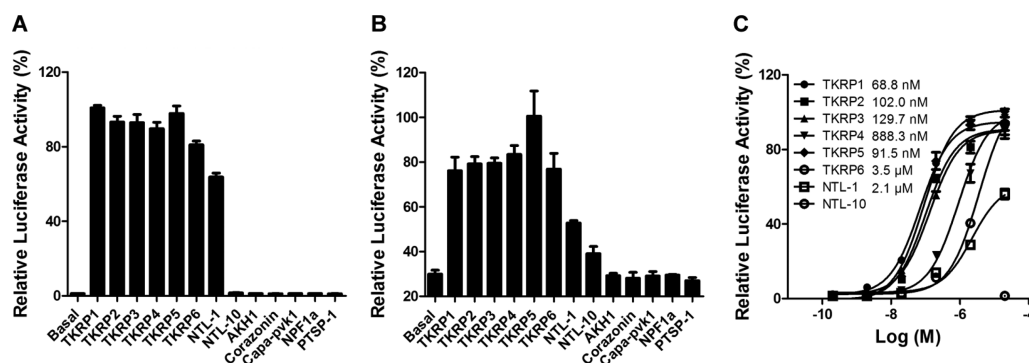


**Figure 2.** BNHR-A24 is a specific tachykinin-related peptide receptor. (A) Luciferase activities of HEK293 cells expressing BNHR-A24 and the reporter gene pCRE-Luc. Cells were treated with 10  $\mu$ M *B. mori* neuropeptides, and responses were normalized against the maximal responses. Abbreviations: TKRP, tachykinin-related peptide; NTL, natalisin; AKH, adipokinetic hormone; NPF, neuropeptide F; PTSP-1, prothoracicostatic peptide. (B) Sf21 cells transiently transfected with BNHR-A24 and the reporter gene pBmCRE-Luc were treated with 10  $\mu$ M *Bombyx* neuropeptides for 4 h, followed by detection of luciferase activities. (C) Dose–response curves of HEK293 cells stably expressing BNHR-A24 and the reporter gene pCRE-Luc treated with *Bombyx* TKRPs. All data were taken from at least three independent experiments.

(TAATAC GACTCA CTATAG GGCG). dsRNAs were synthesized *in vitro* using a MEGascript T7 Kit (Ambion) according to the manufacturer's instructions using the sense primer 5'-TAATAC GACTCA CTATAG GGCGGG AAACCT GGTGT CATCTG GAT-3 and the antisense primer 5'-TAATAC GACTCA CTATAG GGCGCT GGAG-TA TCGGTA GGTCAT CG-3'. Phenol/chloroform extraction followed by ethanol precipitation was used to purify the dsRNA. The dsRNA was diluted in nuclease-free water to the desired concentration (final volume of 2–5  $\mu$ L) and injected into the abdomen of larvae on the second day of the fifth larval instar using a 10  $\mu$ L microsyringe. dsRNA derived from the control template pTRI-Xef from the MEGascriptRNAi kit was used as a control. Twenty synchronized fifth instar P50 larvae were used in each trial. After injection, the larvae were maintained under normal conditions and weighed every 24 h until pupation occurred. The leaves and silkworm droppings were collected before and after feeding each day and dehydrated at 95  $^{\circ}$ C for 3 h, followed by separate weighing.

**Quantitative Reverse Transcriptase Polymerase Chain Reaction (Q-RT-PCR).** DNase treatment, cDNA synthesis of various tissues of fifth larval instar p50 silkworm, and primer design were conducted as described previously.<sup>29</sup> Possible contamination of genomic DNA of each total RNA sample was excluded by treatment with the RNase-free DNase according to the manufacturer's instructions (Qiagen) and subsequently confirmed by detecting Actin A3 mRNA levels in RNA samples using PCR. First-strand cDNA was synthesized using the PrimeScript 1st Strand cDNA Synthesis Kit (Takara) according to the manufacturer's instructions. RT-PCR amplification mixtures (20  $\mu$ L) contained 20 ng of template cDNA, 2 $\times$  SYBR Green I Master Mix buffer (10  $\mu$ L) (Takara), and 400 nM forward and reverse primer (listed in Table S1 of the Supporting Information). The Q-RT-PCR was conducted using a real-time PCR instrument (CFX-touch, Bio-Rad). A melt curve analysis, performed at the end of the PCR cycles, confirmed the specificity of primer annealing. For each pair of primers, the melt curve displayed a single sharp peak. The specificity of the primers was further verified by both gel electrophoresis and sequencing of the PCR products. To ensure the quality of the measurements, a duplicate, no template control and a positive control were included in every run for each primer pair. Standard curves, with a series of

diluted spiked plasmid cDNA as the template, were established to determine the reaction efficiency for all the primer pairs. Results were expressed using the comparative cycle threshold ( $\Delta\Delta$ Ct) method as described previously.<sup>30</sup> Briefly, data were normalized by subtracting the Ct value of the geometric average of the reference genes GAPDH, Rp49, RpL3, and Actin A3 from that of the target gene. The  $\Delta\Delta$ Ct was calculated as the difference in the normalized Ct value ( $\Delta$ Ct) of the different tissue samples. The comparative expression level of target genes is equal to  $2^{-\Delta\Delta$ Ct}. The qPCRs were performed in duplicate with three biological replicates.

## RESULTS

**Cloning and Expression of the Putative Tachykinin Receptor.** BNHR-A24 was grouped into the same cluster as the tachykinin-like receptor by genomic and phylogenetic analysis.<sup>16,25</sup> The full-length cDNA sequence encoding BNHR-A24 (GenBank accession number NM\_001134250) was obtained by RT-PCR from brain tissue of silkworm larvae. As showed in Figure 1A, an alignment between BNHR-A24 and five reported tachykinin-like receptor protein sequences was performed. The amino acid sequence of BNHR-A24 is 43.0, 34.3, 36.3, 30, and 30.3% identical with those of *D. melanogaster* DTKR, *Stomoxys calcitrans* STKR, human NK-1, human NK-2, and human NK-3 receptors, respectively. Specifically, the transmembrane regions are the parts of the receptor that show the highest degree of similarity. To verify the correct expression and localization in a heterogeneous expression system, a chimera of the receptor with the enhanced green fluorescent protein (EGFP) fused to the C-terminus was constructed and was stably or transiently expressed in HEK293 and Sf21 cells. Confocal microscopy revealed that BNHR-A24-EGFP was mainly expressed and localized to the plasma membrane with some intracellular accumulation in the absence of the ligand in both HEK293 and Sf21 cells (Figure 1B,C).

**BNHR-A24 Is Specifically Activated by TKRPs.** To examine the interactions of BNHR-A24 with *Bombyx* peptide ligands, a reporter gene system using a pCRE-luc construct consisting of the firefly luciferase coding region under the control of a minimal promoter containing cAMP response elements was constructed. HEK293 and Sf21 cells expressing BNHR-A24 and pCRE-luc were established for functional assays. The *Bombyx* TKRPs and natalisin-1 (NTL-1) (Table S2

of the Supporting Information) induced a significant increase in luciferase activities in HEK293-BNGR-A24 and Sf21-BNGR-A24 cells, as illustrated in panels A and B of Figure 2, whereas other *Bombyx* neuropeptides, including adipokinetic hormone 1 (AKH1), Corazonin, Capa-pv1, neuropeptide F1 (NPF1), prothoracicostic peptide 1 (PTSP-1), and natalisin-10 (NTL-10), did not produce any detectable responses at a concentration of 10  $\mu\text{M}$ . As a control, no change in the CRE-driven luciferase activity was detected in parental HEK293 and Sf21 cells (Figure S1 of the Supporting Information). An additional dose-dependent assay showed that TKRP1 and TKRP5 appeared to be the most active ligands, while NTL-1 demonstrated only partial activity on BNGR-A24 with a  $B_{\text{max}}$  much lower than that of TKRPs (Figure 2C).

In addition to the cAMP response, HEK293-BNGR-A24 cells exhibited a rapid response in  $\text{Ca}^{2+}$  mobilization when they were challenged with 1  $\mu\text{M}$  *Bombyx* TKRPs and NTL-1. As indicated in Figure 3A, TKRPs elicited an increase in the

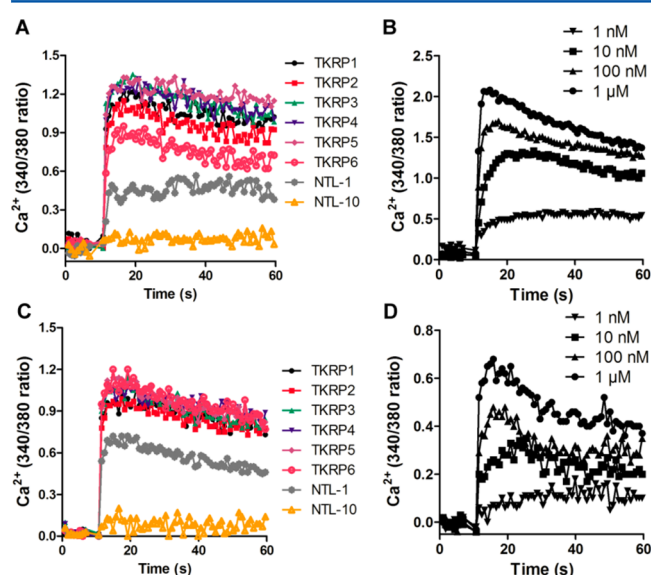


**Figure 3.** Calcium response of BNGR-A24 to *Bombyx* TKRPs or natalisin peptides. (A) HEK293 cells stably expressing BNGR-A24 were exposed to 1  $\mu\text{M}$  *Bombyx* TKRPs or natalisin peptides. HEK293-BNGR-A24 cells were loaded with fura-2, and fluorescence was recorded after stimulation with neuropeptides. (B) Fura-2 ratio of BNGR-A24-expressing HEK293 cells in response to various concentration of *Bombyx* TKRP1 from 1 nM to 1  $\mu\text{M}$ . (C) Sf21-BNGR-A24 cells were loaded with fura-2 and exposed to 1  $\mu\text{M}$  *Bombyx* neuropeptides. The fluorescence was recorded after stimulation with neuropeptides. (D) Dose-response analysis of calcium mobilization in Sf21-BNGR-A24 cells stimulated with TKRP1. All data were taken from at least three independent experiments.

intracellular  $\text{Ca}^{2+}$  concentration in HEK293-BNGR-A24 cells, while NTL-1 showed much lower activity on BNGR-A24. Notable responses were also detected in Sf21-BNGR-A24 cells by *Bombyx* TKRPs (Figure 3C). A dose-dependent response of the intracellular  $\text{Ca}^{2+}$  concentration was further recorded in HEK293-BNGR-A24 and Sf21-BNGR-A24 cells by TKRP1 (Figure 3B,D).

**BNGR-A24 Is Directly Activated by TKRPs.** To confirm the direct interaction of BNGR-A24 with TKRP peptides, ligand competitive binding assays were conducted with a synthesized Cy5-tagged TKRP5 at the N-terminus (Cy5-

TKRP5). The functional assay indicated that Cy5-TKRP5 could activate BNGR-A24 with an  $\text{EC}_{50}$  of 824.9 nM in HEK293 cells (Figure 4A). No significant binding of Cy5-TKRP5 in AKHR-transfected cells was observed (Figure S2 of the Supporting Information). The displacement of Cy5-TKRP5 with TKRPs in HEK293-BNGR-A24 cells was measured by FACS analysis. As shown in panels B and C of Figure 4, a significant block of binding of Cy5-TKRP5 to BNGR-A24 was detected by unlabeled TKRPs, but not by 1  $\mu\text{M}$  *Bombyx* AKH1 (Figure S2 of the Supporting Information). Additionally, displacement curves were constructed using various concentrations of TKRP1 and TKRP5 (Figure 4D,E). The observed inhibition constant ( $K_i$ ) values for TKRP1 and TKRP5 were 10.4 and 11.5 nM in HEK293-BmTKRPR and 34.9 and 5.6 nM in Sf21-BmTKRPR cells, respectively. These  $K_i$  values for TKRP1 and TKRP5 are within the range of  $\text{EC}_{50}$  values for the activation of BNGR-A24. These competition binding analyses further demonstrated that *Bombyx* TKRPs directly bind and activate BNGR-A24. On the basis of these results, we designate BNGR-A24 as BmTKRPR.

**BmTKRPR Signals via  $G_s$ - and  $G_q$ -Dependent Pathways.** Additional functional assays with specific inhibitors were introduced to assess the detailed BmTKRPR-mediated signaling pathways. As shown in panels A and B of Figure 5, upon stimulation with TKRP1, an increase in the intracellular cAMP level in BmTKRPR-expressing HEK293 and Sf21 cells was detected using a direct cAMP ELISA kit. In addition, cholera toxin (CT) preincubation, which ADP-ribosylates and activates  $G_s$  subunit proteins, led to a significant impairment in the BmTKRPR-mediated increase in luciferase activity, thus indicating that  $G_s$  protein is likely involved in BmTKRPR-mediated signaling (Figure 5C). In addition, specific siRNA-mediated knockdown of  $G_s$  protein resulted in a significant decrease in the luciferase activity evoked by TKRP1, confirming the role of  $G_s$  in the TKRP-mediated activation of BNGR-A24 (Figure 5D,E). Moreover, preincubation with the  $G_q$  inhibitor UBO-QIC, a compound analogous to YM-254890,<sup>31</sup> and the PLC inhibitor U73122 led to a significant decrease in the level of intracellular  $\text{Ca}^{2+}$  mobilization (Figure 5F,G), suggesting the involvement of  $G_q$  protein in BmTKRPR-mediated  $\text{Ca}^{2+}$  mobilization. Taken together, these results suggest that the BmTKRPR in both HEK293 and Sf21 cells was specifically activated by *Bombyx* TKRPs by dually coupling to the  $G_s$  and  $G_q$  protein, leading to intracellular cAMP accumulation and  $\text{Ca}^{2+}$  mobilization.

***Bombyx* TKRPs Activate the ERK1/2 Signaling Pathway via BmTKRPR.** Next, the ERK1/2 phosphorylation mediated by BmTKRPR was further assessed. As shown in panels A and C of Figure 6, treatment of BNGR-A24-expressing cells with *Bombyx* TKRP1 elicited transient activation of ERK1/2, with maximal phosphorylation evident at 5 min in HEK293 cells and 10 min in Sf21 cells. Further dose-dependent analysis indicated that the response of BNGR-A24 to TKRP1 had an  $\text{EC}_{50}$  value of 4.7 nM in HEK293 cells (Figure 6B) and 112.6 pM in Sf21 cells (Figure 6D).

Moreover, diverse specific inhibitors were used to further characterize BmTKRPR-mediated ERK1/2 activation in HEK293 cells. HEK293-BmTKRPR cells were treated with TKRP1 in the presence or absence of the PKA inhibitors H89 and KT5720, the  $G_q$  inhibitor UBO-QIC, the PLC inhibitor U73122, and the MEK inhibitor U0126. As shown in Figure 7A–D, I, H89, KT5720, UBO-QIC, U73122, and U0126, respectively, led to significant decreases in the level of

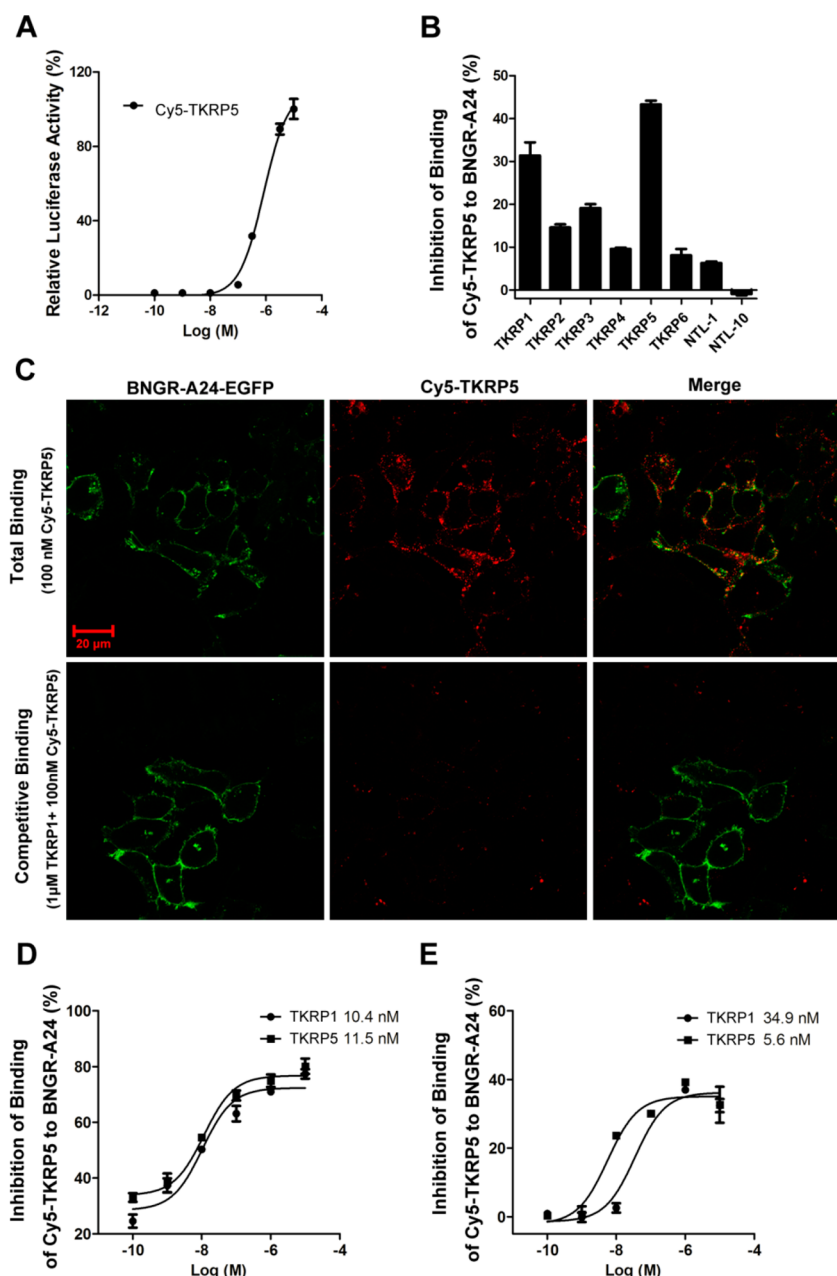


**Figure 4.** Inhibition of binding of Cy5-TKRPs to BNGR-A24 by *Bombyx* TKRPs. (A) Luciferase activity of HEK293 cells stably expressing BNGR-A24 and the reporter gene pCRE-Luc in response to various concentrations of Cy5-TKRPs. (B) Competition binding analyses. Binding of Cy5-TKRPs to HEK-BNGR-A24 cells was measured in the absence of unlabeled peptides (total binding) or in the presence of 1  $\mu$ M unlabeled *Bombyx* TKRPs. The fluorescence intensity was detected by flow cytometry. The extent of binding was determined by fluorescence intensity and is presented as a percentage of the total binding. (C) Binding of Cy5-TKRPs to HEK293-BNGR-A24 cells in the absence of the unlabeled peptide (total binding) or in the presence of unlabeled TKRP1 visualized by confocal microscopy. (D and E) Binding of the Cy5-TKRPs to HEK-BNGR-A24 cells (D) and Sf21-BNGR-24 cells (E) measured in the absence of unlabeled peptides (total binding) or in the presence of increasing concentrations of unlabeled *Bombyx* TKRP1 and TKRP5. All data were taken from at least three independent experiments.

BmTKRPR-mediated ERK1/2 phosphorylation, suggesting that both the  $G_s$  and  $G_q$  pathways were involved in BmTKRPR-mediated ERK1/2 activation. This finding prompted us to investigate whether PKC is involved in BmTKRPR-mediated signaling. As illustrated in Figure 7E–H, the intracellular calcium chelator BAPTA-AM and the calcium-sensitive PKC inhibitor Go6976 had no effect on TKRP1-induced ERK1/2 phosphorylation, whereas treatment with the broad spectrum PKC inhibitor GF109203X and Go6983 led to a significant inhibition of BmTKRPR-mediated ERK1/2 activation, suggest-

ing that a calcium-insensitive PKC is likely to participate in  $G_q$ -coupled BmTKRPR-mediated ERK1/2 activation. These results confirmed that BmTKRPR signals to ERK1/2 via  $G_s$  and  $G_q$  dually coupled pathways in response to TKRP1.

**Expression and dsRNA-Mediated Knockdown of BmTKRPR in *B. mori*.** To assess the physiological role of BmTKRPR in *Bombyx* larvae, we first examined the tissue distribution of BmTKRPR in different tissues dissected from the fifth instar larvae by quantitative and semiquantitative RT-PCR. As shown in Figure 8A, a high level of BmTKRPR

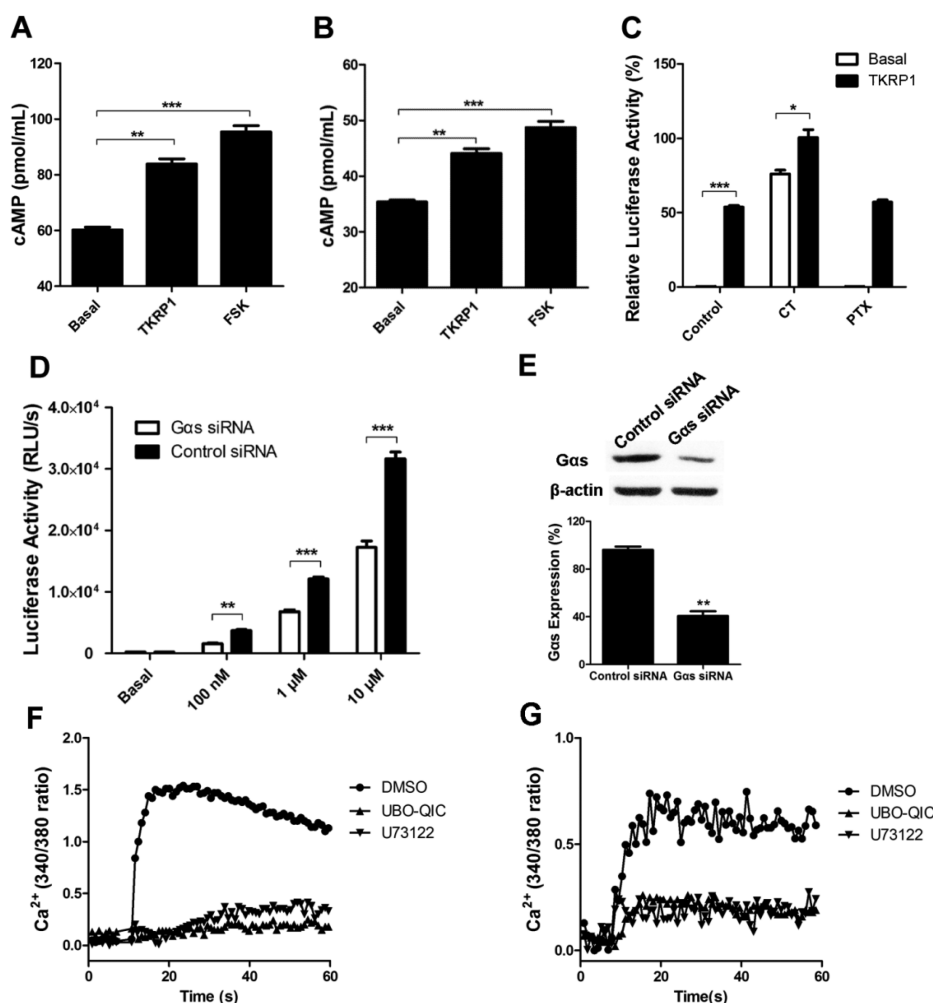


**Figure 5.** BmTKRPR activated by TKRPs via the  $G_s$  and  $G_q$  pathway. (A and B) Accumulation of cAMP in HEK293-BmTKRPR (A) and Sf21-BmTKRPR (B) cells in response to TKRP1. Cells were pretreated with the PDE1 inhibitor IBMX for 1 h followed by stimulation with 100 nM TKRP1 or 10  $\mu$ M forskolin (FSK), and the cAMP level was determined by the cAMP immunoassay detection kit. (C) Effect of cholera toxin (CT) and pertussis toxin (PTX) on luciferase activities of HEK293-BmTKRPR cells in response to 100 nM TKRP1. HEK293-BmTKRPR cells were preincubated with 100 ng/mL CT for 2 h or 50 ng/mL PTX for 16 h, followed by stimulation with 100 nM TKRP1 for 4 h. (D) siRNA-mediated knockdown of  $G_s$  on the luciferase activities evoked by TKRP1. HEK293 cells were transfected with specific  $G_s$  siRNA or control siRNA (Santa Cruz). Twenty-four hours later, the cells were seeded on a six-well plate and transiently transfected with BmTKRPR and pCRE-luc. The luciferase activities were determined as described in Materials and Methods. (E)  $G_s$  expression was detected with a specific  $G_s$  antibody (Santa Cruz) by Western blotting. Seventy-two hours after transfection, cells were harvested, and equal amounts of total cellular lysate were separated by 10% SDS-PAGE and incubated with the indicated antibody. The levels of  $G_s$  expression were normalized to  $\beta$ -actin, and all immunoblots were quantified using the Bio-Rad Quantity One imaging system. (F and G) Calcium rise induced by TKRP1 in  $G_q$  inhibitor UBO-QIC or PLC $\beta$  inhibitor U73122-treated (U73122) and nontreated (DMSO) cells. HEK293-BmTKRPR (F) and Sf21-BmTKRPR (G) cells were pretreated with the  $G_q$  inhibitor UBO-QIC or PLC inhibitor U73122 (5  $\mu$ M) for 30 min prior to the treatment with 100 nM TKRP1. All data were taken from at least three independent experiments.

expression was detected in the brain, midgut, and testis of the silkworm larvae. We also observed relatively obvious expression of BmTKRPR in the Malpighian tubule, fat body, and ovary, thereby suggesting multifunctional features of this receptor.

A previous study demonstrated that injection of the *Bombyx* tachykinin-related peptide resulted in a shorter latency period, suggesting a possible stimulatory effect on feeding.<sup>32</sup> Accordingly, RNAi-mediated knockdown of BmTKRPR was accomplished through injection of dsRNA at the beginning of the fifth instar. As shown in Figure 8B, the mRNA levels of BmTKRPR on day 3 of the fifth instar were significantly suppressed in the larval brain and midgut compared to the controls. The amount of food consumed, the amount of food digested, and the coefficient of digestibility [digestibility = (leaf weight of

consumption – silkworm dropping)/leaf weight of consumption  $\times$  100%]<sup>33</sup> as well as the body weight were further measured to monitor the growth situation of the silkworms. As illustrated in panels C and D of Figure 8, the dsRNA-mediated knockdown of BmTKRPR led to a significant decrease in body weight and digestibility but exerted no effect on the total food consumed (data not show). Those data further suggested that BmTKRPR is likely involved in the regulation of feeding and growth.

## DISCUSSION

Insect TKRPs were identified more than two decades ago;<sup>2</sup> however, relatively few corresponding receptors have been fully characterized. In *B. mori*, three orphan GPCRs, BNGR-A24,

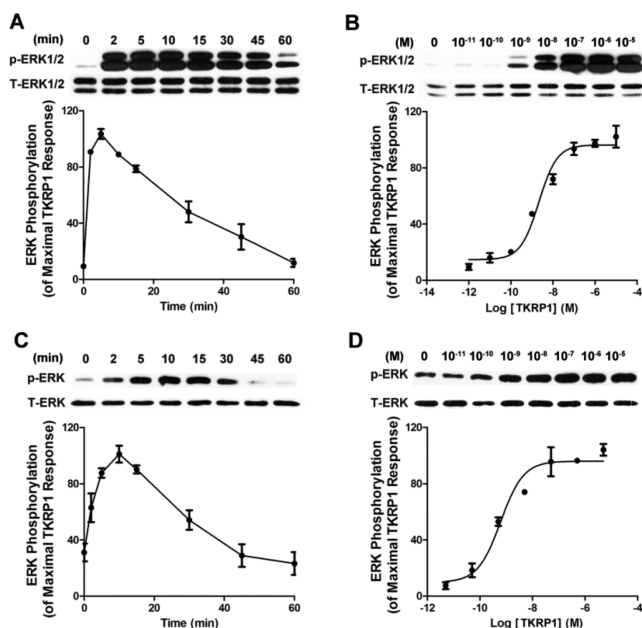


**Figure 6.** *Bombyx* tachykinin-related peptide receptor BmTKRPR mediates MAPK/ERK pathway activation. HEK293 cells stably expressing BmTKRPR were starved with serum-free medium for 1 h prior to the addition of ligands. (A) Kinetics of ERK1/2 phosphorylation initiated by TKRP1 in HEK293-BmTKRPR cells. Serum-starved cells were stimulated with 100 nM TKRP1 for the indicated periods of time and harvested to detect ERK1/2 phosphorylation. Values indicate the percentage of the maximal response by TKRP1. (B) Dose response of analysis of ERK1/2 phosphorylation on HEK293-BmTKRPR cells. Serum-starved cells were incubated with an increasing dose of TKRP1, ranging from 10 pM to 10  $\mu$ M, for 5 min and harvested to detect ERK1/2 phosphorylation. (C) Kinetics of ERK1/2 phosphorylation initiated by TKRP1 in Sf21-BmTKRPR cells. (D) Dose-dependent analysis of ERK1/2 phosphorylation on Sf21-BmTKRPR cells. All data were taken from at least three independent experiments.

BNGR-A32, and BNGR-A33, have been identified *in silico* as putative tachykinin receptors.<sup>16,25,26</sup> Most recently, natalisin, a group of neuropeptides considered to be an ancestral sibling of tachykinin, was identified from *B. mori* and was paired with orphan GPCRs, BNGR-A32 and BNGR-A33.<sup>27</sup> In the study presented here, using functional assays and a fluorescence labeling peptide-based binding assay, BNGR-A24 was found to be directly activated by all six *Bombyx* TKRPs carrying the FX<sub>1</sub>GX<sub>2</sub>R/Ka consensus sequence, with a high affinity in both HEK293 and Sf21 cells, but not by any other *Bombyx* neuropeptides, such as AKH1, Capa-pvk1, Corazonin, NPF, sNPF, and PTSP-1. *Bombyx* neuropeptide NTL-1 carrying the FxxxRa consensus sequence also exhibited a lower activity on BNGR-A24-expressing cells. Together with the data on TKRPs-mediated ERK1/2 phosphorylation, our findings demonstrated that BNGR-A24 was specifically activated by synthetic TKRPs with high activity (full agonists) and synthetic NTL-1 with low and partial activity (partial agonist). Therefore, BNGR-A24 is more appropriately designated as a *Bombyx* tachykinin-related peptide receptor (BmTKRPR).

Although *Drosophila* DTKR was shown to interact with the pertussis toxin-sensitive G<sub>i/o</sub> protein when it was functionally expressed in *Xenopus* oocytes,<sup>19</sup> when using HEK293 or *Drosophila* Schneider 2 (S2) cells, DTKR clearly stimulated a dose-dependent increase in both intracellular Ca<sup>2+</sup> and cAMP

levels upon exposure to *Drosophila* tachykinin-related peptides.<sup>23,24</sup> Likewise, the stable fly tachykinin receptor, STKR, was also shown to elicit a transient increase in intracellular Ca<sup>2+</sup> levels, as well as an increase in the level of intracellular cAMP formation.<sup>21,34</sup> In this study, the *Bombyx* TKRP receptor being expressed in both HEK293 and Sf21 cells was activated by TKRPs, resulting in a significant increase in intracellular cAMP levels that was sensitive to treatment with the G<sub>s</sub> constitutive activator cholera toxin. We also observed that treatment with TKRPs elicited a rapid increase in intracellular Ca<sup>2+</sup> concentration in a dose-dependent manner, and this activation was completely blocked by the G<sub>q</sub> inhibitor UBO-QIC and the PLC inhibitor U73122. Moreover, BmTKRPR-mediated ERK1/2 phosphorylation was significantly blocked by the PKA inhibitors H89 and KT5720, as well as the G<sub>q</sub> inhibitor UBO-QIC. Taken together, these data demonstrated that the *Bombyx* TKRP receptor dually couples to G<sub>s</sub> and G<sub>q</sub> proteins, activating both the PLC/Ca<sup>2+</sup> and AC/cAMP signaling pathways.

It is well-known that activated GPCRs signal to the mitogen-activated protein kinase (MAPK) cascades via distinct G<sub>i</sub>-, G<sub>s</sub>-, and G<sub>q</sub>-dependent signaling pathways, leading to the phosphorylation of ERK1/2, which is known to regulate diverse processes ranging from proliferation and differentiation to apoptosis.<sup>35</sup> In the study presented here, our data demonstrate that BmTKRPR-mediated phosphorylation of ERK1/2 was significantly inhibited by the PKA inhibitor H89, suggesting the involvement of the G<sub>s</sub>/cAMP/PKA cascade in the regulation of BmTKRPR-induced ERK1/2 activation. Furthermore, our investigation showed that BmTKRPR-mediated ERK1/2 activation was effectively blocked by the PLC inhibitor U73122 and the broad spectrum PKC inhibitors Go6983 and GF109203X, but not by the intracellular calcium chelator BAPTA-AM or the calcium-sensitive PKC inhibitor Go6976, suggesting a possible role of the calcium-insensitive PKC in the BmTKRPR-mediated activation of ERK1/2. It is now accepted that the DAG-PKC signaling pathway has been well conserved throughout evolution from yeast to humans, and in even a relatively simple organism, the nematode worm *Caenorhabditis elegans*.<sup>36</sup> It seems likely that the activation of the G<sub>q</sub> protein-coupled BmTKRPR causes an increase in phospholipase C (PLC) activity, resulting in the hydrolysis of phosphatidylinositol 4,5-bisphosphate [PtdIns(4,5)P<sub>2</sub>] and subsequent generation of diacylglycerol,<sup>37</sup> which in turn activates PKC.<sup>38</sup> PKC subsequently activates raf-1 by stimulating the formation of active Ras–Raf-1 complexes, leading to the activation of the ERK1/2 signaling cascade.<sup>39</sup> Our data derived from different inhibitors showed that BmTKRPR-induced ERK1/2 activation was partially blocked following treatment with PKA inhibitors H89 and KT5720 but almost completely abrogated by UBO-QIC. It is likely that G<sub>q</sub> and G<sub>s</sub> dually coupled BmTKRPR exhibited a predominantly G<sub>q</sub>-mediated and to a lesser extent a G<sub>s</sub>-mediated ERK1/2 phosphorylation, which was consistent with the observations with cannabinoid CB2 receptor mutant CB2-P139L<sup>40</sup> and G<sub>q</sub>-, G<sub>s</sub>-, and G<sub>i</sub>-coupled orexin receptor-1 (OX1R) by Ramanjaneya et al.<sup>41</sup> In addition, we demonstrated that although UBO-QIC exhibited no inhibitory effect on forskolin, a direct activator of adenylate cyclase, and induced activation of ERK1/2, the G<sub>s</sub> protein activator cholera toxin (CT)-initiated ERK1/2 activation was attenuated by UBO-QIC (Figure S3 of the Supporting Information), suggesting that the off-target inhibition effect on G<sub>s</sub> protein is likely to contribute

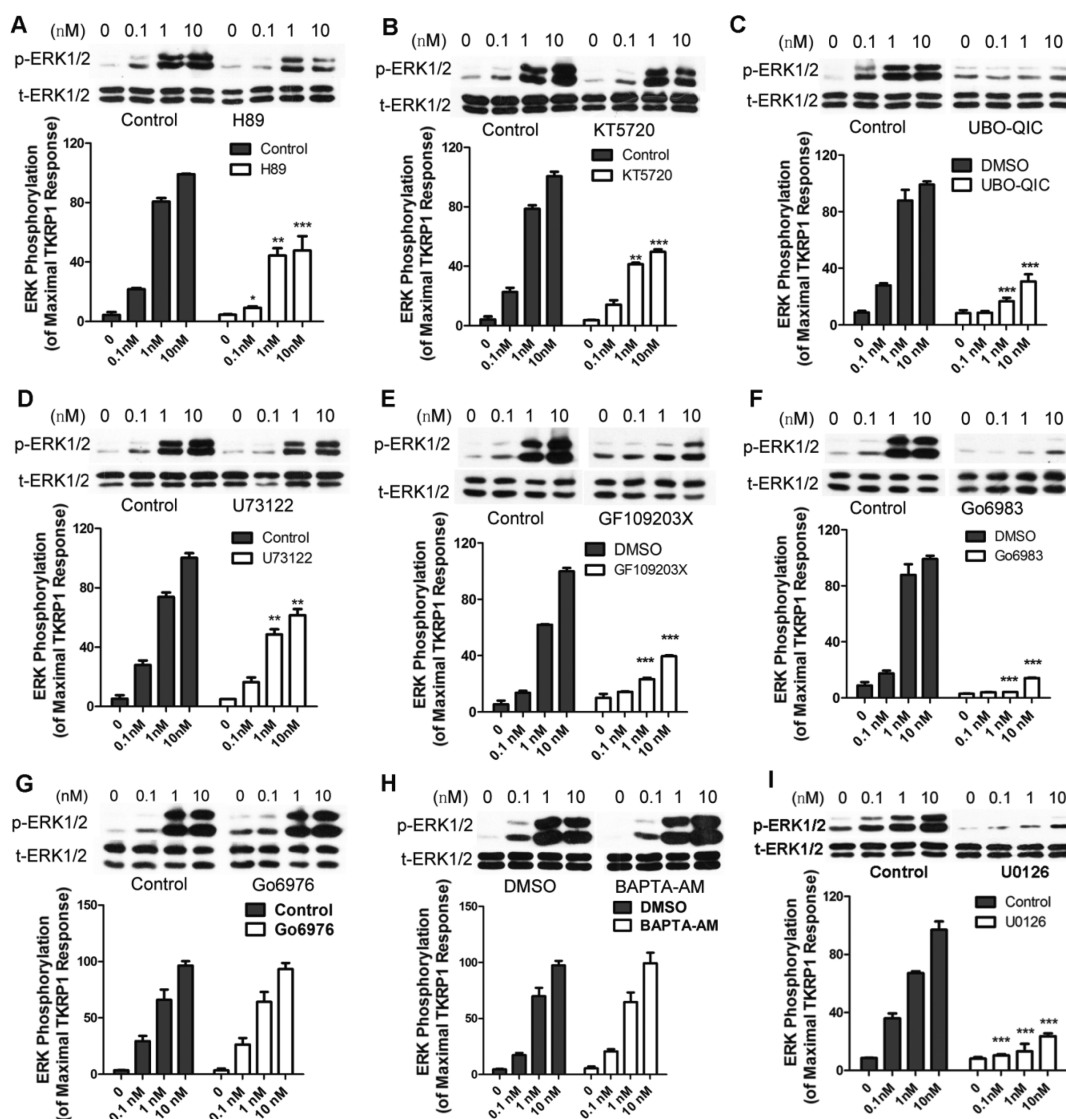


**Figure 7.**  $G_q$ /PLC $\beta$ /PKC and  $G_s$ /cAMP/PKA were involved in BmTKRPR-mediated ERK1/2 phosphorylation. HEK293 cells stably expressing BmTKRPR were starved with serum-free medium for 1 h prior to the addition of ligands. Serum-starved cells were pretreated with vehicle (DMSO) or drugs [(A) 10  $\mu$ M H89, (B) 1  $\mu$ M KT5720, (C) 1  $\mu$ M UBO-QIC, (D) 5  $\mu$ M U73122, (E) 10  $\mu$ M GF109203x, (F) 10  $\mu$ M Go6983, (G) 1  $\mu$ M Go6976, (H) 20  $\mu$ M BAPTA-AM, or (I) 1  $\mu$ M U0126] for 1 h and then stimulated by the indicated concentrations of TKRP1 for 5 min. Cells were harvested to detect ERK1/2 phosphorylation. Data were analyzed by using a Student's *t* test (\*\**p* < 0.01; \*\*\**p* < 0.001). All data were taken from at least three independent experiments.

to the UBO-QIC-caused inhibition of ERK1/2 phosphorylation.

In this study, two cell expression systems, mammalian cell line HEK293 and insect cell line Sf21, were used for functional characterization of BmTKRPR/NTL receptors, and interestingly, our results showed that *Bombyx* TKRPs exhibited different activities in the CRE-Luc-based cAMP assay between the HEK293 cell system and the Sf21 cell system. Analysis of ERK1/2 phosphorylation by Western blotting demonstrated that *Bombyx* TKRPs displayed relatively higher activities in BmTKRPR-expressing Sf21 cells than in BmTKRPR-expressing HEK293 cells. Previous studies also revealed that the functional response of an insect neuropeptide receptor can be influenced by the type of expression system.<sup>42</sup> The exact reason leading to different responses of *Bombyx* TKRPs in HEK293 and Sf21 cells is unknown. Perhaps differences in posttranslational modifications,<sup>43–45</sup> the cholesterol content of the cell membranes,<sup>46–48</sup> and cultural conditions<sup>49</sup> or unrecognized

differences between HEK293 and Sf21 cells could be responsible for these discrepancies. Thus, a better defined homologous expression system with a cellular context that is closer to the natural physiological situation is to be preferred for a physiologically relevant characterization of insect neuropeptide receptors.

It is well-established that tachykinins exert various physiological and even pathological effects in the peripheral and central nervous systems. TK-like neuropeptides from the CNS of the locust *Lo. migratoria* were originally characterized as myotropic peptides.<sup>1,2</sup> The first identified insect tachykinin-related neuropeptide receptor DTKR was found to be involved in the regulation of locomotor activity, insulin signaling, and olfactory sensory processing in the antennal lobe.<sup>50–52</sup> A few studies also established that TKRPs played a role in a weak diuretic action on the renal tubules of moth and locust,<sup>53,54</sup> in feeding and metabolism, and in stress.<sup>32,55</sup> In the meantime, our results revealed that dsRNA-mediated knockdown of

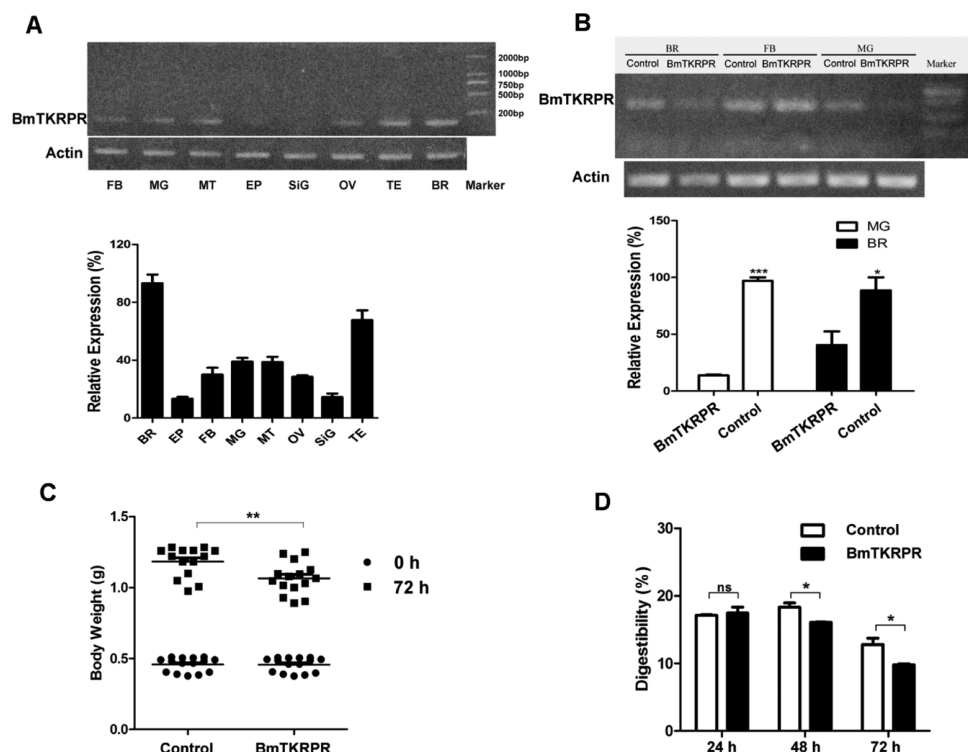


**Figure 8.** BmTKRPR expression in tissues and the effects of dsRNA-mediated knockdown of BNGR-A24 on growth. (A) mRNA expression of BmTKRPR in tissues of day 3 larvae of fifth instar was analyzed by semiquantitative RT-PCR (top) and quantitative RT-PCR (below) and normalized to the geometric mean of four reference genes (GAPDH, Rpl3, Rpl49, and actin A3). Abbreviations: BR, brain; EP, epidermis; FB, fat body; MG, midgut; MT, Malpighian tube; OV, ovary; SiG, silk gland; TE, testis. (B) Effects of dsRNA injection on BNGR-A24 expression in BR and MG. BmTKRPR dsRNA (10  $\mu$ g) or control dsRNA (pTRI-Xef from the kit) was injected on the second day of fifth instar larvae. BNGR-A24 gene expression was determined by semiquantitative RT-PCR (top) and quantitative RT-PCR (below) 48 h after injection. (C) Effects of BmTKRPR dsRNA treatment on silkworm body weight. After injection, silkworms were fed with mulberry leaves every 8 h and weighed every 24 h. (D) Effects of dsRNA treatment on silkworm digestibility. Digestibility = (leaf weight of consumption – silkworm dropping)/leaf weight of consumption  $\times$  100%. All data were taken from at least three independent experiments, and data were analyzed using a Student's *t* test (\**p* < 0.05; \*\**p* < 0.01; \*\*\**p* < 0.001).

BmTKRPR resulted in a significant loss of weight and precocious metamorphosis, suggesting the possible physiological role of the BmTKRPR receptor in the regulation of food intake and growth. However, in mammals, central and peripheral administration of SP acutely suppresses feeding behavior in rats and chicks, suggesting vertebrate tachykinin may function as endogenous anorexigenic peptides.<sup>56,57</sup> The difference between invertebrate TKRPs and vertebrate tachykinin on feeding behavior needs to be elucidated further. Moreover, further quantitative and semiquantitative RT-PCR analysis showed that a high level of BmTKRPR expression occurred in the brain, midgut, and testis of fifth instar larvae, and the relatively lower level of BmTKRPR expression was also detectable in tissues of the Malpighian tubule, fat body, and ovary, consistent with the observations of Yamanaka et al.<sup>26</sup> and indicating that the TKRP system is likely to function as a pleiotropic regulator. Therefore, further efforts should be focused on the molecular and functional dissection of the physiological roles of the *Bombyx* TKRP system.

In conclusion, we have identified the *Bombyx* orphan receptor BNGR-A24 as a specific receptor for the *Bombyx* tachykinin-related peptide. Upon direct interaction with a peptide agonist, the *Bombyx* TKRP receptor couples to  $G_s$  and  $G_q$  proteins and triggers both PLC/ $Ca^{2+}$ /PKC and AC/cAMP/PKA signaling pathways. Additionally, functional analysis using dsRNA-mediated knockdown of BmTKRPR suggested a likely

role of TKRPs and the authentic receptor in the regulation of silkworm feeding and growth. However, more experiments using RNAi or other manipulations *in vivo* are required to further elucidate the mechanism(s) involving in insect TKRP system-mediated regulation of fundamental physiological processes.

## ■ ASSOCIATED CONTENT

### ● Supporting Information

List of primers (Table S1), amino acid sequence of *B. mori* TKRPs and natalisin (Table S2), *B. mori* TKRP-mediated luciferase activities in vehicle cells (Figure S1), binding of Cy5-TKR5 to vehicle cells (Figure S2), and activity of  $G_s$  protein that was partially affected by  $G_q$  inhibitor UBO-QIC (Figure S3). This material is available free of charge via the Internet at <http://pubs.acs.org>.

## ■ AUTHOR INFORMATION

### Corresponding Authors

\*College of Life Sciences, Zhejiang University, Zijingang Campus, 866 Yuhang Tang Rd., Hangzhou 310058, China. Telephone: +86-571-88206748. Fax: +86-571-88206134-8000. E-mail: znm2000@yahoo.com.

\*Key Laboratory of Genetic Improvement of Sericulture, Ministry of Agriculture, Jiangsu University of Science and

Technology, Zhenjiang, Jiangsu 212018, China. Telephone: +86-511-85616539. E-mail: zgzsri@163.com.

# Funding

This work was supported by grants from the National Natural Science Foundation of China (31172150, 31272375, and 31301881) and the Ministry of Science and Technology of China (2012CB910402).

# Notes

The authors declare no competing financial interest.

# ACKNOWLEDGMENTS

We thank Aiping Shao, Ming Ding, and Hanmin Chen for their technical assistance and equipment usage.

# ABBREVIATIONS

TKRP, tachykinin-related peptide; NTL, natalisin; TKRPR, tachykinin-related peptide receptor; BNGR, *B. mori* neuro-peptide receptor; GPCR, G protein-coupled receptor; EGFP, enhanced green fluorescent protein; CRE, cAMP response element.

# REFERENCES

- (1) Schoofs, L., Holman, G. M., Hayes, T. K., Kochansky, J. P., Nachman, R. J., and De Loof, A. (1990) Locustatachykinin III and IV: Two additional insect neuropeptides with homology to peptides of the vertebrate tachykinin family. *Regul. Pept.* 31, 199–212.
- (2) Schoofs, L., Holman, G. M., Hayes, T. K., Nachman, R. J., and De Loof, A. (1990) Locustatachykinin I and II, two novel insect neuropeptides with homology to peptides of the vertebrate tachykinin family. *FEBS Lett.* 261, 397–401.
- (3) Muren, J. E., and Nassel, D. R. (1996) Isolation of five tachykinin-related peptides from the midgut of the cockroach *Leucophaea maderae*: Existence of N-terminally extended isoforms. *Regul. Pept.* 65, 185–196.
- (4) Muren, J. E., and Nassel, D. R. (1997) Seven tachykinin-related peptides isolated from the brain of the Madeira cockroach: Evidence for tissue-specific expression of isoforms. *Peptides* 18, 7–15.
- (5) Lundquist, C. T., Clottens, F. L., Holman, G. M., Nichols, R., Nachman, R. J., and Nassel, D. R. (1994) Callitachykinin I and II, two novel myotropic peptides isolated from the blowfly, *Calliphora vomitoria*, that have resemblances to tachykinins. *Peptides* 15, 761–768.
- (6) Meola, S. M., Clottens, F. L., Holman, G. M., Nachman, R. J., Nichols, R., Schoofs, L., Wright, M. S., Olson, J. K., Hayes, T. K., and Pendleton, M. W. (1998) Isolation and immunocytochemical characterization of three tachykinin-related peptides from the mosquito, *Culex salinarius*. *Neurochem. Res.* 23, 189–202.
- (7) Winther, A. M., Siviter, R. J., Isaac, R. E., Predel, R., and Nassel, D. R. (2003) Neuronal expression of tachykinin-related peptides and gene transcript during postembryonic development of *Drosophila*. *J. Comp. Neurol.* 464, 180–196.
- (8) Takeuchi, H., Yasuda, A., Yasuda-Kamatani, Y., Kubo, T., and Nakajima, T. (2003) Identification of a tachykinin-related neuropeptide from the honeybee brain using direct MALDI-TOF MS and its gene expression in worker, queen and drone heads. *Insect Mol. Biol.* 12, 291–298.
- (9) Satake, H., and Kawada, T. (2006) Overview of the primary structure, tissue-distribution, and functions of tachykinins and their receptors. *Curr. Drug Targets* 7, 963–974.
- (10) Scherckenbeck, J., and Zdobinsky, T. (2009) Insect neuropeptides: Structures, chemical modifications and potential for insect control. *Bioorg. Med. Chem.* 17, 4071–4084.
- (11) Broeck, J. V. (2001) Insect G protein-coupled receptors and signal transduction. *Arch. Insect Biochem. Physiol.* 48, 1–12.
- (12) Nassel, D. R. (2002) Neuropeptides in the nervous system of *Drosophila* and other insects: Multiple roles as neuromodulators and neurohormones. *Prog. Neurobiol.* 68, 1–84.

- (13) Coast, G. M., and Garside, C. S. (2005) Neuropeptide control of fluid balance in insects. *Ann. N.Y. Acad. Sci.* 1040, 1–8.
- (14) Predel, R., Neupert, S., Roth, S., Derst, C., and Nassel, D. R. (2005) Tachykinin-related peptide precursors in two cockroach species. *FEBS J.* 272, 3365–3375.
- (15) Van Loy, T., Vandersmissen, H. P., Poels, J., Van Hiel, M. B., Verlinden, H., and Vanden Broeck, J. (2010) Tachykinin-related peptides and their receptors in invertebrates: A current view. *Peptides* 31, 520–524.
- (16) Roller, L., Yamanaka, N., Watanabe, K., Daubnerova, I., Zitnan, D., Kataoka, H., and Tanaka, Y. (2008) The unique evolution of neuropeptide genes in the silkworm *Bombyx mori*. *Insect Biochem. Mol. Biol.* 38, 1147–1157.
- (17) Gan, L., Liang, J., Liu, X., and He, N. (2010) Neuropeptide gene screening and mature peptide prediction in the silkworm, *Bombyx mori*. *Kunchong Xuebao* 53, 11.
- (18) Liu, X., Ning, X., Zhang, Y., Chen, W., Zhao, Z., and Zhang, Q. (2012) Peptidomic Analysis of the Brain and Corpora Cardiaca-Corpora Allata Complex in the *Bombyx mori*. *Int. J. Pept.* 2012, 640359.
- (19) Li, X. J., Wolfgang, W., Wu, Y. N., North, R. A., and Forte, M. (1991) Cloning, heterologous expression and developmental regulation of a *Drosophila* receptor for tachykinin-like peptides. *EMBO J.* 10, 3221–3229.
- (20) Monnier, D., Colas, J. F., Rosay, P., Hen, R., Borrelli, E., and Maroteaux, L. (1992) NKD, a developmentally regulated tachykinin receptor in *Drosophila*. *J. Biol. Chem.* 267, 1298–1302.
- (21) Guerrero, F. D. (1997) Cloning of a cDNA from stable fly which encodes a protein with homology to a *Drosophila* receptor for tachykinin-like peptides. *Ann. N.Y. Acad. Sci.* 814, 310–311.
- (22) Johard, H. A., Muren, J. E., Nichols, R., Larhammar, D. S., and Nassel, D. R. (2001) A putative tachykinin receptor in the cockroach brain: Molecular cloning and analysis of expression by means of antisera to portions of the receptor protein. *Brain Res.* 919, 94–105.
- (23) Birse, R. T., Johnson, E. C., Taghert, P. H., and Nassel, D. R. (2006) Widely distributed *Drosophila* G-protein-coupled receptor (CG7887) is activated by endogenous tachykinin-related peptides. *J. Neurobiol.* 66, 33–46.
- (24) Poels, J., Verlinden, H., Fichna, J., Van Loy, T., Franssens, V., Studzian, K., Janecka, A., Nachman, R. J., and Vanden Broeck, J. (2007) Functional comparison of two evolutionary conserved insect neurokinin-like receptors. *Peptides* 28, 103–108.
- (25) Fan, Y., Sun, P., Wang, Y., He, X., Deng, X., Chen, X., Zhang, G., and Zhou, N. (2010) The G protein-coupled receptors in the silkworm, *Bombyx mori*. *Insect Biochem. Mol. Biol.* 40, 581–591.
- (26) Yamanaka, N., Yamamoto, S., Zitnan, D., Watanabe, K., Kawada, T., Satake, H., Kaneko, Y., Hiruma, K., Tanaka, Y., Shinoda, T., and Kataoka, H. (2008) Neuropeptide receptor transcriptome reveals unidentified neuroendocrine pathways. *PLoS One* 3, e3048.
- (27) Jiang, H., Lkhagva, A., Daubnerova, I., Chae, H. S., Simo, L., Jung, S. H., Yoon, Y. K., Lee, N. R., Seong, J. Y., Zitnan, D., Park, Y., and Kim, Y. J. (2013) Natalisin, a tachykinin-like signaling system, regulates sexual activity and fecundity in insects. *Proc. Natl. Acad. Sci. U.S.A.* 110, E3526–E3534.
- (28) Yang, H., He, X., Yang, J., Deng, X., Liao, Y., Zhang, Z., Zhu, C., Shi, Y., and Zhou, N. (2013) Activation of cAMP-response element-binding protein is positively regulated by PKA and calcium-sensitive calcineurin and negatively by PKC in insect. *Insect Biochem. Mol. Biol.* 43, 1028–1036.
- (29) Vandesompele, J., De Preter, K., Pattyn, F., Poppe, B., Van Roy, N., De Paepe, A., and Speleman, F. (2002) Accurate normalization of real-time quantitative RT-PCR data by geometric averaging of multiple internal control genes. *Genome Biol.* 3, RESEARCH0034.
- (30) Livak, K. J., and Schmittgen, T. D. (2001) Analysis of relative gene expression data using real-time quantitative PCR and the  $2^{-\Delta\Delta C_T}$  Method. *Methods* 25, 402–408.
- (31) Fujioka, M., Koda, S., Morimoto, Y., and Biemann, K. (1988) Structure of FR900359, a cyclic depsipeptide from *Ardisia crenata* Sims. *J. Org. Chem.* 53, 2820–2825.

- (32) Nagata, S., Morooka, N., Matsumoto, S., Kawai, T., and Nagasawa, H. (2011) Effects of neuropeptides on feeding initiation in larvae of the silkworm, *Bombyx mori*. *General and Comparative Endocrinology* 172, 90–95.
- (33) Waldbauer, G. (1968) The consumption and utilization of food by insects. *Adv. Insect Physiol.* 5, 229–288.
- (34) Torfs, H., Shariatmadari, R., Guerrero, F., Parmentier, M., Poels, J., Van Poyer, W., Swinnen, E., De Loof, A., Akerman, K., and Vanden Broeck, J. (2000) Characterization of a receptor for insect tachykinin-like peptide agonists by functional expression in a stable *Drosophila* Schneider 2 cell line. *J. Neurochem.* 74, 2182–2189.
- (35) Rozengurt, E. (2007) Mitogenic signaling pathways induced by G protein-coupled receptors. *J. Cell. Physiol.* 213, 589–602.
- (36) Mellor, H., and Parker, P. J. (1998) The extended protein kinase C superfamily. *Biochem. J.* 332 (Part 2), 281–292.
- (37) Weiss, A., Irving, B. A., Tan, L. K., and Koretzky, G. A. (1991) Signal transduction by the T cell antigen receptor. *Semin. Immunol.* 3, 313–324.
- (38) Nishizuka, Y. (2003) Discovery and prospect of protein kinase C research: Epilogue. *J. Biochem.* 133, 155–158.
- (39) Marais, R., Light, Y., Mason, C., Paterson, H., Olson, M. F., and Marshall, C. J. (1998) Requirement of Ras-GTP-Raf complexes for activation of Raf-1 by protein kinase C. *Science* 280, 109–112.
- (40) Zheng, C., Chen, L., Chen, X., He, X., Yang, J., Shi, Y., and Zhou, N. (2013) The second intracellular loop of the human cannabinoid CB2 receptor governs G protein coupling in coordination with the carboxyl terminal domain. *PLoS One* 8, e63262.
- (41) Ramanjaneya, M., Conner, A. C., Chen, J., Kumar, P., Brown, J. E., Johren, O., Lehnert, H., Stanfield, P. R., and Randeva, H. S. (2009) Orexin-stimulated MAP kinase cascades are activated through multiple G-protein signalling pathways in human H295R adrenocortical cells: Diverse roles for orexins A and B. *J. Endocrinol.* 202, 249–261.
- (42) Claeys, I., Poels, J., Simonet, G., Franssens, V., Van Loy, T., Van Hiel, M. B., Breugelmans, B., and Vanden Broeck, J. (2005) Insect neuropeptide and peptide hormone receptors: Current knowledge and future directions. *Vitam. Horm.* 73, 217–282.
- (43) Kuroda, K., Geyer, H., Geyer, R., Doerfler, W., and Klenk, H. D. (1990) The oligosaccharides of influenza virus hemagglutinin expressed in insect cells by a baculovirus vector. *Virology* 174, 418–429.
- (44) Zhang, R., Cai, H., Fatima, N., Buczko, E., and Dufau, M. L. (1995) Functional glycosylation sites of the rat luteinizing hormone receptor required for ligand binding. *J. Biol. Chem.* 270, 21722–21728.
- (45) Gutierrez, J., Kremer, L., Zaballos, A., Goya, I., Martinez, A. C., and Marquez, G. (2004) Analysis of post-translational CCR8 modifications and their influence on receptor activity. *J. Biol. Chem.* 279, 14726–14733.
- (46) Gimpl, G., Klein, U., Reilander, H., and Fahrenholz, F. (1995) Expression of the human oxytocin receptor in baculovirus-infected insect cells: High-affinity binding is induced by a cholesterol-cyclodextrin complex. *Biochemistry* 34, 13794–13801.
- (47) Beukers, M. W., Klaassen, C. H., De Grip, W. J., Verzijl, D., Timmerman, H., and Leurs, R. (1997) Heterologous expression of rat epitope-tagged histamine H2 receptors in insect Sf9 cells. *Br. J. Pharmacol.* 122, 867–874.
- (48) Colozo, A. T., Park, P. S., Sum, C. S., Pisterzi, L. F., and Wells, J. W. (2007) Cholesterol as a determinant of cooperativity in the M2 muscarinic cholinergic receptor. *Biochem. Pharmacol.* 74, 236–255.
- (49) Schneider, E. H., and Seifert, R. (2010) Sf9 cells: A versatile model system to investigate the pharmacological properties of G protein-coupled receptors. *Pharmacol. Ther.* 128, 387–418.
- (50) Winther, A. M., Acebes, A., and Ferrus, A. (2006) Tachykinin-related peptides modulate odor perception and locomotor activity in *Drosophila*. *Mol. Cell. Neurosci.* 31, 399–406.
- (51) Ignell, R., Root, C. M., Birse, R. T., Wang, J. W., Nassel, D. R., and Winther, A. M. (2009) Presynaptic peptidergic modulation of olfactory receptor neurons in *Drosophila*. *Proc. Natl. Acad. Sci. U.S.A.* 106, 13070–13075.
- (52) Birse, R. T., Soderberg, J. A., Luo, J., Winther, A. M., and Nassel, D. R. (2011) Regulation of insulin-producing cells in the adult *Drosophila* brain via the tachykinin peptide receptor DTKR. *J. Exp. Biol.* 214, 4201–4208.
- (53) Johard, H. A., Coast, G. M., Mordue, W., and Nassel, D. R. (2003) Diuretic action of the peptide locustatachykinin I: Cellular localisation and effects on fluid secretion in Malpighian tubules of locusts. *Peptides* 24, 1571–1579.
- (54) Skaer, N. J., Nassel, D. R., Maddrell, S. H., and Tublitz, N. J. (2002) Neurochemical fine tuning of a peripheral tissue: Peptidergic and aminergic regulation of fluid secretion by Malpighian tubules in the tobacco hawkmoth *M. sexta*. *J. Exp. Biol.* 205, 1869–1880.
- (55) Kahsai, L., Kapan, N., Dirksen, H., Winther, A. M., and Nassel, D. R. (2010) Metabolic stress responses in *Drosophila* are modulated by brain neurosecretory cells that produce multiple neuropeptides. *PLoS One* 5, e11480.
- (56) Tachibana, T., Khan, M. S., Matsuda, K., Ueda, H., and Cline, M. A. (2010) Central administration of substance P inhibits feeding behavior in chicks. *Horm. Behav.* 57, 203–208.
- (57) Dib, B. (1999) Food and water intake suppression by intracerebroventricular administration of substance P in food- and water-deprived rats. *Brain Res.* 830, 38–42.